High Temp. Mater. Proc., Vol. **30** (2011), pp. 77–80 DOI 10.1515/HTMP.2011.010

Optical and Thermal Behaviors of Polyamide-Layered Silicate Nanocomposites Based on 4,4'-Azodibenzoic Acid by Solution Intercalation Technique

Khalil Faghihi[1,*] **and Meisam Shabanian**[1]

[1] Organic Polymer Research Laboratory, Department of Chemistry, Faculty of Science Arak University, Arak, Iran

Abstract. Two new samples of polyamide-montmorillonite reinforced nanocomposites based on 4,4'-azodibenzoic acid were prepared by a convenient solution intercalation technique. Polyamide (PA) **4** as a source of polymer matrix was synthesized by the direct polycondensation reaction of 4,4'-azodibenzoic acid **2** with 4,4'-diamino diphenyl sulfone **3** in the presence of triphenyl phosphate (TPP), $CaCl_2$, pyridine and N-methyl-2-pyrrolidone (NMP). Morphology and structure of the resulting PA-nanocomposite films **4a** and **4b** with 10 and 20 % silicate particles were characterized by FTIR spectroscopy, X-ray diffraction (XRD) and scanning electron microscopy (SEM). The effect of clay dispersion and the interaction between clay and polymeric chains on the properties of nanocomposite films were investigated by using Uv-vis spectroscopy, thermogravimetric analysis (TGA) and water uptake measurements.

Keywords. 4,4'-azodibenzoic acid, polyamide-montmorillonite nanocomposite, optical and thermal properties.

1 Introduction

Polymer-clay nanocomposites typically exhibited mechanical, thermal and gas barrier properties, which are superior to those of the corresponding pure polymers [1–6]. Unique properties of the nanocomposites are usually observed when the ultra fine silicate layers are homogenously dispersed throughout the polymer matrix at nanoscale. The uniform dispersion of silicate layers is usually desirable for maximum reinforcement of the materials. Due to the incompatibility of hydrophilic layered silicates and hydrophobic polymer matrix, the individual nanolayers are not easily separated and dispersed in many polymers. For this purpose, silicate layers are usually modified with an intercalating agent to obtain organically modified clay prior to use in nanocomposite formation [7–11]. Also aromatic polyamides are one of the most important classes of high performance polymers, because they posses excellent mechanical properties, thermal stability, chemical resistance and low flammability and are good substitutes for ceramics and metals in the automotive, aerospace, and microelectronic industries [12–14]. In this article two new PA-nanocomposite films with 10 and 20 % silicate particles containing 4,4'-azodibenzoic acid moiety in the main chain were prepared by using a convenient solution intercalation technique.

Corresponding author: Khalil Faghihi, Organic Polymer Research Laboratory, Department of Chemistry, Faculty of Science Arak University, Arak 38156-8-8449, Iran; E-mail: k-faghihi@araku.ac.ir.

Received: August 22, 2010. Accepted: September 17, 2010.

2 Experiments

2.1 Materials

4-Nitrobenzoic acid, glucose, 4,4'-diamino diphenyl sulfone, triphenyl phosphate (TPP), $CaCl_2$, pyridine and N-methyl-2-pyrrolidone (NMP) were purchased from Merck Chemical Company and used without previous purification.

2.2 Measurements

Fourier transform infrared (FTIR) spectra were recorded on Galaxy Series FTIR 5000 spectrophotometer (England). UV-visible spectra were recorded at 298 K (25 °C) in the 250–700 nm spectral regions with a Perkin Elmer Lambda 15 spectrophotometer in NMP solution using cell lengths of 1 cm. Thermal Gravimetric Analysis (TGA and DTG) data were taken on a Mettler TA4000 System under N_2 atmosphere at a rate of 10 °C/min. The morphology of nanocomposite film was investigated on Cambridge S260 scanning electron microscope (SEM). X-ray diffraction (XRD) were performed on Philips X-Pert (Cu-Ka radiation, $\lambda = 0.15405$ nm). The water absorption of PA-nanocomposite films were carried out using a procedure under ASTM D570–81 [15].

2.3 Monomer Synthesis

4,4'-Aazodibenzoic acid **2** was prepared according to a typical procedure shown in scheme 1 [16].

2.4 Polymer Synthesis

Into a 100 mL round bottomed flask were placed a mixture of 4,4'-azodibenzoic acid **2** (0.002 mol), 4,4'-diamino diphenyl sulfone **3** (0.002 mol), 0.60 g of calcium chloride, 1.0 mL of triphenyl phosphite, 1.0 mL of pyridine and 4.0 mL NMP. The mixture was heated for 1 h at 333 K (60 °C), 2 h at 363 K (90 °C) and then refluxed at 403 K (130 °C) for 8 h until a viscous solution was formed. Then it was cooled at room temperature and 30 mL of methanol was added to reaction mixture. The precipitate was formed, filtered off and washed with methanol. The resulting polymer **4** was dried under vacuum. The inherent viscosity of this soluble PA **4** was 0.45 dL/g.

2.5 PA-Nanocomposite Synthesis 4a and 4b

PA-nanocomposites **4a** and **4b** were produced by solution intercalation method, in two different amounts of organoclay particles (10 and 20-mass %). The appropriate amounts of PA solution in N-methyl-2-pyrrolidone (NMP) were mixed to yield particular nanocomposite concentrations. To control the dispersibility of organoclay in polyamide matrix, constant stirring was applied at 298 K (25 °C) for 24 h. Nanocomposite films were cast by pouring the solutions for each concentration into Petri dishes placed on a leveled surface followed by the evaporation of solvent at 368 K (70 °C) for 12 h. Films were dried at 80 °C under vacuum to a constant weight.

3 Results and Discussion

3.1 Polymer Synthesis

Polyamide **4** was synthesized by the direct solution polycondensation reaction of an equimolar mixture of diacid **2**, an equimolar mixture of diamine **3** by using triphenyl phosphate (TPP) and pyridine as condensing agents (Figure 1). PA **4** was obtained in good yield (96 %) and inherent viscosity (0.45 m^3/kg). The structure of resulting polymer **4** was confirmed as PA by using FTIR spectroscopy and elemental analyses. The resulting polymer has absorption band at 1637 cm^{-1} due to amide carbonyl group. Also absorption band of amide group appeared at 3412 cm^{-1} (N-H stretching). The elemental analysis value of the resulting polymer was in good agreement with the calculated values for the proposed structure.

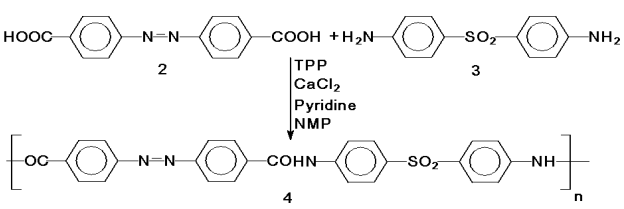

Figure 1. Synthetic route of PA 4.

3.2 PA-Nanocomposite Films Characterization

PA-nanocomposite films were transparent and yellowish brown in color. The incorporation of organoclay changed the color of films to dark yellowish brown. Moreover, a decrease in the transparency was observed at higher clay contents. FT-IR spectroscopy spectra of PA-nanocomposite films **4a** and **4b** showed the characteristic absorption bands of the Si-O and Mg-O moieties at 1038, 515 and 465 cm^{-1} respectively. The incorporation of organic groups in PAnanocomposite films was confirmed by the presence of peaks at 1770, 1720, 1380, 720 cm^{-1} (imide rings) and 1670 cm^{-1} (amide carbonyl group). Figure 2 shows the XRD patterns of PA-nanocomposite films **5a** and **5b** containing 10 and 20 mass % of silicate particles. These results indicated significant expansion of the silicate layer after insertion PA chains. The shift in the diffraction peaks PA-nanocomposite films confirms that intercalation has been taken place. This is direct evidence that PA-nanocomposites have been formed as the nature of intercalating agent also affects the organoclay dispersion in the polymer matrix. In our PA- nanocomposite films there are coherent XRD signal at 5.75° and 4.20° related to 10 and 20 mass % nanocomposite films respectively.

The surface morphology of the PA-nanocomposite films prepared by solution intercalation technique is compared by SEM analyses (Figure 3). The SEM images show that PA matrix has a smooth morphology, where as the PA matrix has amorph morphology. Also SEM micrographs of PA-nanocomposite containing 10 and 20 mass % clay platelets were uniformly distributed without agglomeration.

Optical clarity of PA-nanocomposite films containing 10 and 20 wt. % clay platelets and neat PA was compared by Uv-vis spectroscopy in the region of 260–800 nm (Figure 4). These spectra show that the UV-visible region (260–800 nm) is affected by the presence of the clay particles and

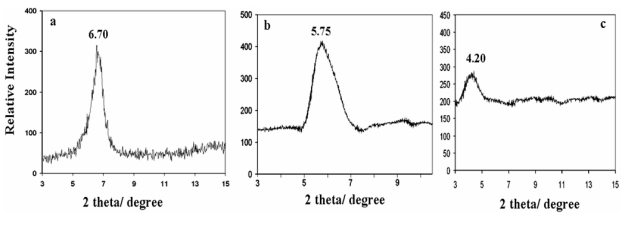

Figure 2. X-ray diffraction patterns of Organoclay (a), PA-nanocomposite films 4a (b) and 4b (c).

Polyimide	T_5 (°C)[a]	T_{10} (°C)[b]	Char Yield[c]	Water uptake (%)[d]
4	305	345	47	7.3
4a	320	370	51	5.5
4b	370	405	58	0.5

[a,b] Temperature at which 5 % and 10 % weight loss was recorded by TGA at heating rate of 10 K/min in N_2 respectively, [c] Percentage weight of material left undecomposed after TGA analysis 873 K (600 °C), [d] Percentage weight of material left undecomposed after TGA analysis 873 K (600 °C).

Table 1. Thermal behaviors and Water uptake of neat PA **4** and PA-nanocomposite films **4a** & **4b**.

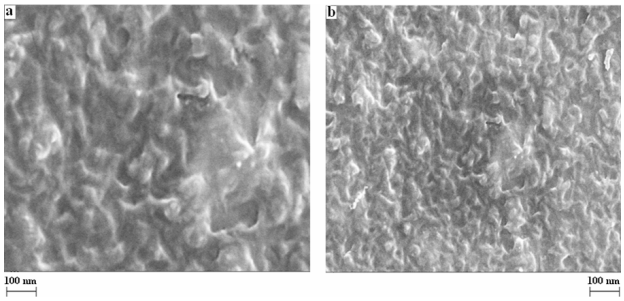

Figure 3. Scanning electron micrographs of PA-nanocomposite films 4a (a) and 4b (b).

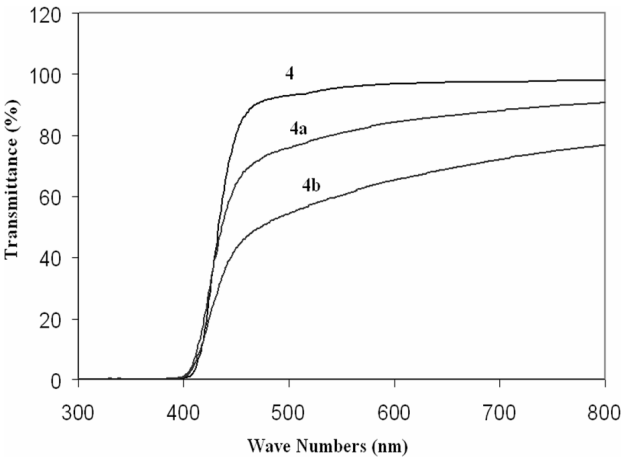

Figure 4. Uv-vis spectra of PA 4, PA-nanocomposite films 4a and 4b.

exhibiting low transparency reflected to the primarily intercalated composites. Results show that the optical clarity of PA-nanocomposite films are significantly lower than the neat PA system.

The PA under investigation contains polar and cyclic imide rings and also polar amide groups in the backbone that have the tendency to uptake water through hydrogen bonding. Thus water absorption measurements become necessary for neat PA **5**, PA-nanocomposite films **4a** and **4b** and data are shown in Table 1. In the water permeability studies, we found that the incorporation of clay platelets into PA matrix results in a decrease of water uptake relative to pure PA by forming the tortuous path of water permeant. Water permeability depends on length, orientation and degree of delaminating of layered silicate [17]. It should be noted that a further increase in clay concentration resulted in an enhanced barrier property of nanocomposites which may be attributed to the plate-like clays that effectively increase the length of the diffusion pathways, as well as decreasing the water permeability.

3.3 Thermogravimetric Analysis

The thermal properties of PA-nanocomposite films containing 10 and 20 wt. % clay platelets and neat PA were investigated by using TGA and DTG in nitrogen atmosphere at heating rate of 10 K/min, and thermal data are summarized in Table 1 (Figure 5). These samples exhibited good resistance to thermal decomposition, up to 573–648 K (300–375 °C) in nitrogen, and began to decompose gradually

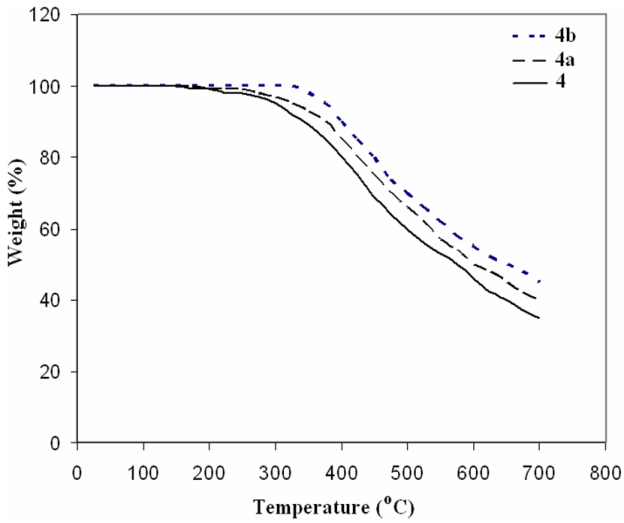

Figure 5. TGA thermograms of neat PA 4 and PA-nanocomposite films 4a and 4.

above this temperature. T_5 for these polymers ranged from 300–375 °C and T_{10} for them ranged from 340–400 °C, and residual weights at 873 K (600 °C) ranged from 46.0 and 55.0 % in nitrogen respectively. Incorporation of organoclay into the PA matrix also enhanced the thermal stability of the nanocomposites.

4 Conclusions

The PA-nanocomposites were successfully prepared using solution intercalation method. The structure and the uniform dispersion of organoclay throughout the PA matrix were confirmed by FTIR, XRD and SEM analyses. The optical clarity and water absorption property of PA-nanocomposites were decreased significantly by increasing the organoclay contents in PA matrix. On the contrary the thermal stability of PA-nanocomposites was increased significantly by increasing the organoclay contents in PA matrix. The enhancements in the thermal stability of the nanocomposites films **4a** and **4b** caused by introducing organoclay may be due to the strong interactions between polymeric matrix and organoclay generating well intercalation and dispersion of clay platelets in the PA matrix.

References

[1] S. Zulfiqar, Z. Ahmad, M. Ishaq, S. Saeed and M. I. Sarwar, *J. Mater. Sci.,* **42** (2007), 93–100.

[2] R. Xu, E. Manias, A. J. Snyder and J. Runt, *Macromolecules,* **34** (2001), 337–339.

[3] A. Kausar, S. Zulfiqar, S. Shabbir, M. Ishaq and M. I. Sarwar, *Polym. Bull.,* **59** (2007), 457–468.

[4] N. Bibi, M. I. Sarwar, M. Ishaq and Z. Ahmad, *Polym. Polym. Compos.,* **15** (2007), 313–319.

[5] T. D. Fornes, P. J. Yoon, H. Keskkula and D. R. Paul, *Polymer,* **42** (2001), 9929–9940.

[6] T. D. Fornes, P. J. Yoon, D. L. Hunter, H. Keskkula and D. R. Paul, *Polymer,* **43** (2002), 5915–5933.

[7] G. M. Chen, Y. M. Ma and Z. N. Qi, *J. Appl. Polym. Sci.,* 77 (2000), 2201–2205.

[8] B. Hoffmann, J. Kressler, G. Stopplemann, C. Friedrich and G. M. Kim, *Colloid Polym. Sci.,* **278** (2000), 629–636.

[9] X. Liu, Q. Wu, Q. Zhang, L. A. Berglund and Z. Mo, *Polym. Bull.,* **48** (2002), 381–387.

[10] R. K. Ayyer and A. I. Leonov, *Rheol. Acta,* **43** (2004), 283–292.

[11] A. B. Morgan and J. W. Gilman, *J. Appl. Polym. Sci.,* **87** (2003), 1329–1338.

[12] P. E. Cassidy, *Thermally Stable Polymers*, Dekker, New York (1980).

[13] H. H. Yang, *Aromatic High-Strength Fibers*, Wiley, New York (1986).

[14] D. J. Liaw, W. H. Chen, and C. C. Huang, *Polyimide and Other High-Temperature Polymers*, VSP (2003).

[15] S. Zulfiqar and M. I. Sarwar, *J. Incl. Phenom. Macrocycl. Chem.,* **62** (2008), 353–361.

[16] K. Faghihi and M. Hajibeygi, *Eur. Polym. J.,* **39** (2003), 2307–2314.

[17] R. K. Bharadwaj, *Macromolecules* 34 (2001), 9189–9192.